

LM-0300 Fabry Perot Spectrum Analyser

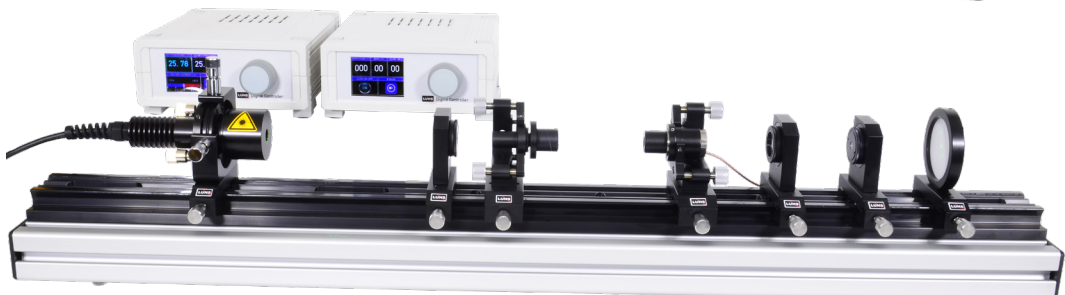
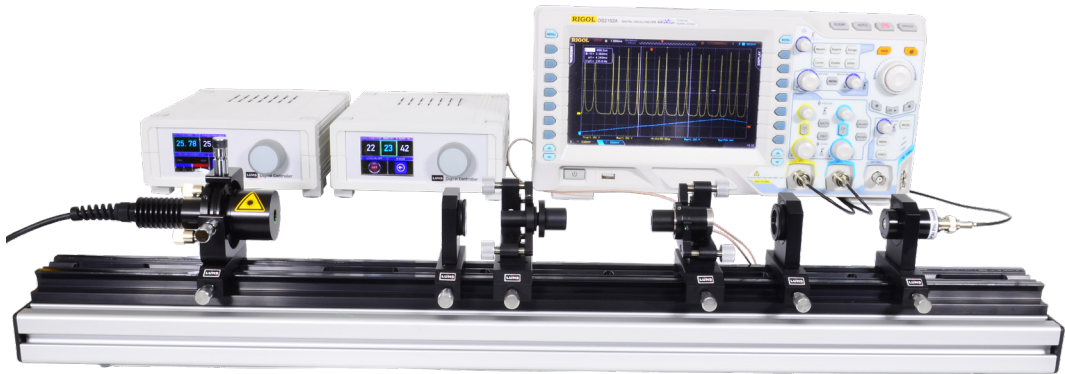
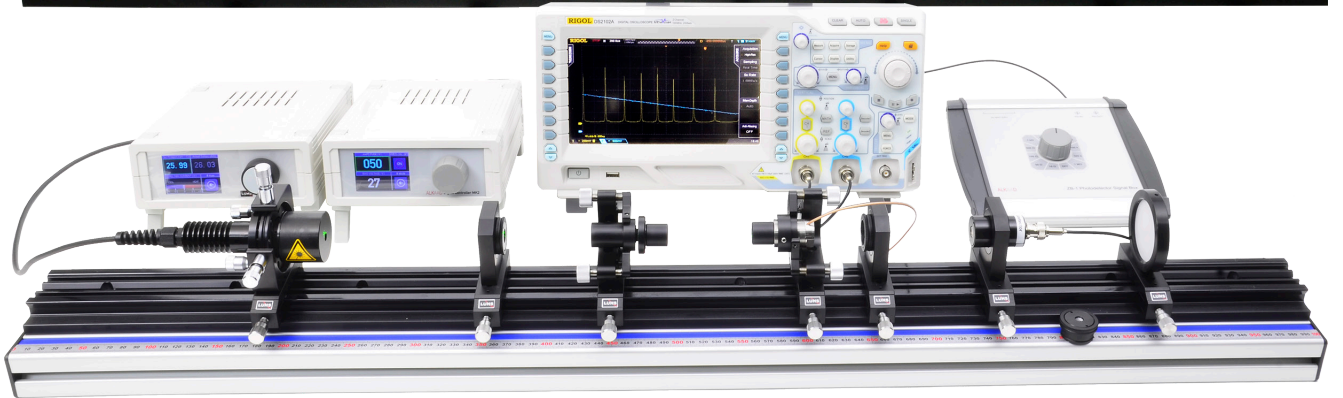
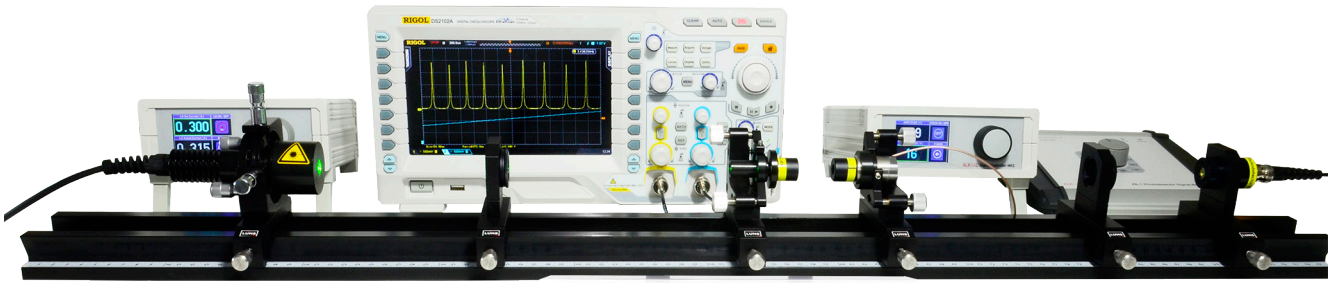


Table of Contents

1.0 INTRODUCTION	3
1.1 The Ideal Fabry Perot	4
1.2 The real Fabry Perot	8
1.3 The Spherical Fabry Perot	8
1.4 The Spherical FP in practice	8
1.5 Optical Stability Criterion	9
2.0 EXPERIMENTAL SETUP	10
2.1 Description of the components	11
3.0 APPLICATION AND MEASUREMENTS	18
3.1 Experiments with the green emitting single mode laser	18
3.1.1 Static measurements	18
3.1.2 Dynamic Measurements	19
3.2 Experiments with the red emitting two mode HeNe laser	20
3.2.1 Static measurements	21
3.2.2 Dynamic Measurements	21

1.0 Introduction

When Theodore Maiman discovered the first laser in 1960 he used a Fabry Perot (FP) for two purposes. Firstly the FP was used for high resolution spectroscopy to explore the underlying energy states of the Ruby material and secondly it served as optical cavity. It is named after Charles Fabry and Alfred Perot, who developed the instrument in 1899.



Charles Fabry



Alfred Perot

Almost each laser needs a FP for the operation, however, in this context it is mainly termed as optical cavity.

This experiment shows the properties of optical resonators especially the „Fabry Perot“ (FP) resonator which is the most important of all stable laser resonators. The properties and behaviour of such a resonator will be discussed and measured as well as the resonance condition, the free spectral range and finesse. The stability criteria of confocal, hemispherical and plane parallel resonator types are calculated and measured. Finally, the resonator will be used as a spectrum analyser, a so called scanning Fabry Perot.

The mode spectra of the provided green single mode diode pumped solid state laser (DPSSL) and optional two mode HeNe-laser is measured. The resonator mirrors are mounted in precision adjustment holders. One mirror is mounted on a low voltage piezoelectric transducer (PZT) which is controlled in amplitude and frequency by means of a voltage (0-50 V) controller. The other one is mounted into a precise translation element to achieve the perfect confocal match for curved mirror. The PZT periodically changes the length (0 to 10 μm) of the cavity sweeping over some resonances. The signal of the photodiode and the triangular PZT scanning amplitude are displayed on an oscilloscope showing the Airy function for some resonances. By using the known distance of the FP mirror, the free spectral range is determined and is used to calibrate the horizontal axis of the oscilloscope as the distance of two recurring peaks (Fig. 2). The mode spectra of the DPSSL - Laser is measured and interpreted by this method. Surprisingly, the green emitting DPSSL emits a very pure single mode if the temperature and injection current are properly controlled. In addition, an optional two mode HeNe probe laser can be used to measure the mode spacing with the SFP. Some parts of this experiment can also be used in connection with the experimental HeNe-Laser, to demonstrate the single mode operation, when an etalon is used inside of its cavity. By tuning it, even the gain profile of the HeNe-laser can be measured.

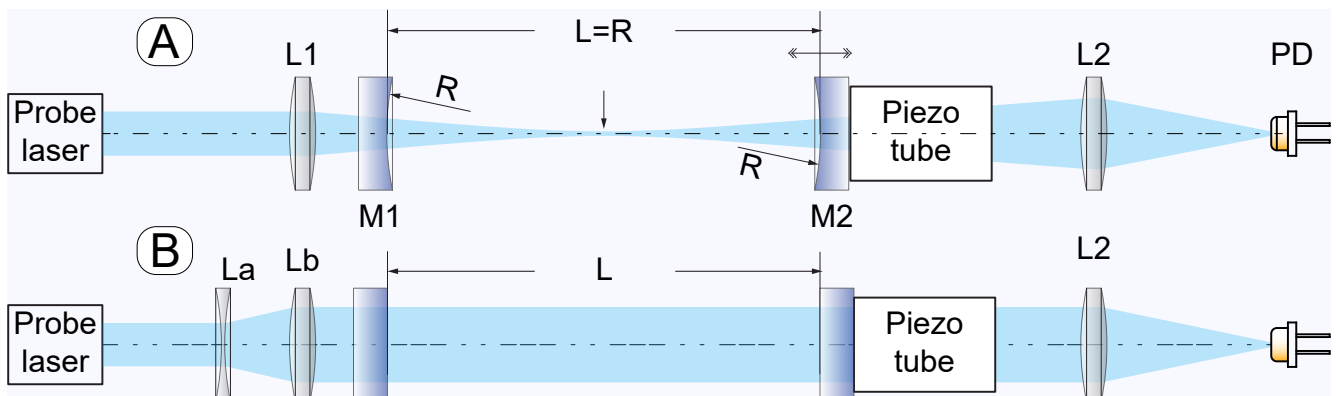


Fig. 1: Spherical and plane Fabry Perot

The classical Fabry Perot (FP) uses two flat mirrors having a fixed distance L to each other. If the mirrors are coated to the surfaces of a highly precise parallel ground and polished glass cylinder such a device is termed as Fabry Perot Etalon. Such a static FP creates a circular interference pattern and its ring structure of it carries the spectral information of the incident light. Another class of a Fabry Perot is the scanning Fabry Perot (SFP). In this case the mirrors are separated, whereby one mirror is mounted to an element which periodically moves the mirror back and forth. The static Airy function which describe the transmittance of a FP becomes now also a function of time t .

$$T = \frac{1}{1 + F \cdot \sin^2\left(\frac{\pi}{\lambda} \cdot n \cdot L\right)} \rightarrow T(t) = \frac{1}{1 + F \cdot \sin^2\left(\frac{\pi}{\lambda} \cdot n \cdot L(t)\right)}$$

F stands for the finesse, λ for the wavelength, n for the index of refraction of the media between the mirror and L as distance of the two mirrors.

The modulation of the length $L(t)$ is usually done with a PZT

the length of which changes depending on the applied voltage. The transmission becomes maximum if the \sin^2 term in the Airy function is zero. This is the case for $L(t) = N\lambda/2$, whereby N is an integer number. The range for $N \rightarrow N+1$ is the range between two consecutive transmission peaks and is called free spectral range (FSR).

$$FSR \rightarrow \delta\nu = \frac{c}{2 \cdot L}$$

We are using $\delta\nu$ as frequency rather than $\delta\lambda$ as wavelength, because it is more convenient. The FSR is a very important value as it allows the calibration of the time axis of the graph of Fig. 2. The finesse F is determined as $FSR/FWHM$ and its value is a parameter for the resolution of the FP. The finesse of a FP depends on the reflectivity of the mirror. However the flatness of the mirrors are even more important. In practice it turns out that the use of flat mirrors creates some disadvantages.

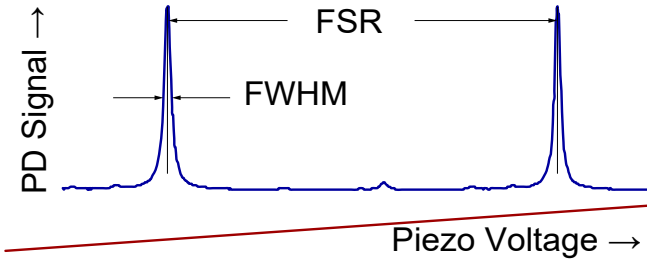


Fig. 2: Typical SFP measurement

Firstly, the alignment of absolute parallelism of both mirrors is hard to achieve and secondly the flatness of the mirror must be very accurate (better than $\lambda/10$). The case (B) of Fig. 1 shows the setup for such a plane mirror SFP. To reduce the limiting effect of the flatness imperfections, the beam of the probe laser is expanded (L_a and L_b). To relax the high demand for precise alignment a SFP with spherical mirror is used. Due to the curved mirror the photons are redirected to stay inside the SFP. For a plane mirror already a small deviation of the parallel aligned mirrors lets the photons leave the cavity after a couple of round trips. In case (A) of Fig. 1 such a spherical SFP is shown. The best results are obtained if the mirror are positioned such, that their distance $L=R$ (confocal). Since mirror M1 acts as concave lens the mode matching lens (L1) compensates this effect. As for all spherical cavities higher transverse modes can occur, thereby falsifying the measurement. The transverse modes vanish if the distance L is exactly aligned to R . For this purpose M1 is mounted onto a precise translation element which can be varied by a few mm.

1.1 The Ideal Fabry Perot

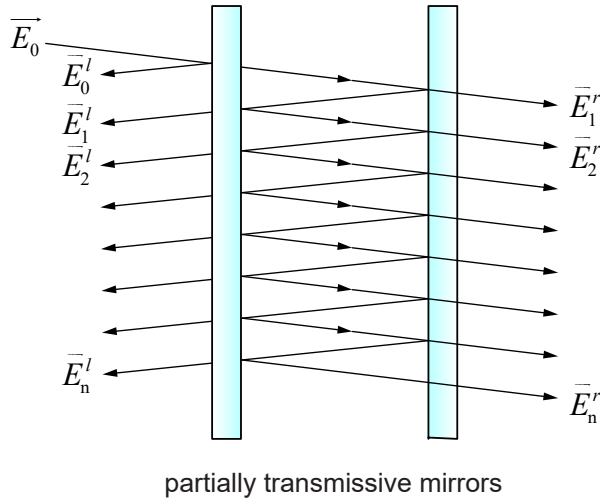


Fig. 3: Fabry and Perot's multi-beam interferometer

The two plates are at a distance d from each other and have a reflectivity R . Absorption should be ignored, resulting in $R = 1-T$ ($T = \text{Transmission}$). The incident light field

$$\vec{E}_0$$

is separated into a manifold of reflected and transmitted field intensities E . The task is to derive a formula which describes the properties of such a Fabry Perot. To make it a bit simpler we start to just consider scalar amplitudes A instead of the field vector E . The wave enters under the angle α the Fabry Perot (from now onwards referred to as FP), (Fig. 4)

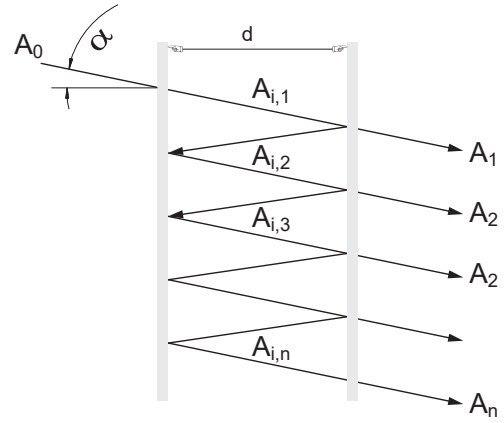


Fig. 4: Figure to derive the individual amplitudes A_n

The incoming wave has the amplitude A_0 and the intensity I_0 . After passing the first plate this intensity is

$$I_1 = (1-R) \cdot I_0 = T \cdot I_0$$

because

$$I = E^2$$

it follows that:

$$A_{i1} = \sqrt{1-R} \cdot A_0$$

$$A_{i2} = R \cdot A_{i1} = \sqrt{1-R} \cdot R^1 \cdot A_0$$

$$A_{i3} = R \cdot A_{i2} = \sqrt{1-R} \cdot R^2 \cdot A_0$$

$$A_{i4} = R \cdot A_{i3} = \sqrt{1-R} \cdot R^3 \cdot A_0$$

$$A_{in} = R \cdot A_{i(n-1)} = \sqrt{1-R} \cdot R^{n-1} \cdot A_0$$

The amplitudes A coming out of the second plate have the values:

$$A_1 = \sqrt{1-R} \cdot A_{i1} = (1-R) \cdot A_0$$

$$A_2 = \sqrt{1-R} \cdot A_{i2} = (1-R) \cdot R^2 \cdot A_0$$

$$A_3 = \sqrt{1-R} \cdot A_{i3} = (1-R) \cdot R^3 \cdot A_0$$

$$A_n = \sqrt{1-R} \cdot A_{in} = (1-R) \cdot R^n \cdot A_0$$

Let us consider in addition the oscillating terms. The following calculation can be made simpler if we use cosine instead of sine.

$$E = A \cdot \cos(\omega t + kx + \delta)$$

δ is the phase shift with reference to E_1 . It is created by passing through many long paths in the FP.

$$\delta = \frac{2kd}{\cos \alpha}$$

$$E_1 = A_1 \cdot \cos(\omega t + kx)$$

$$E_2 = A_2 \cdot \cos(\omega t + kx + \delta)$$

$$E_3 = A_3 \cdot \cos(\omega t + kx + 2 \cdot \delta)$$

$$E_n = A_n \cdot \cos(\omega t + kx + (n-1) \cdot \delta)$$

$$E_n = (1-R) \cdot R^n \cdot A_0 \cdot \cos(\omega t + kx + (n-1) \cdot \delta)$$

The individual field intensities E_n have to be summed up and then squared to obtain the intensity.

$$E = \sum_0^{\infty} E_n$$

To make further derivation easier, we will use the following equation:

$$\cos \gamma = \text{Re}[\cos \gamma - i \cdot \sin \gamma]$$

$\text{Re}[\]$ is the real component of a complex number.

With

$$\cos \gamma = \frac{e^{i\gamma} + e^{-i\gamma}}{2} \quad \text{and} \quad \sin \gamma = \frac{e^{i\gamma} - e^{-i\gamma}}{2i}$$

is

$$\cos \gamma = \text{Re}[e^{i\gamma}]$$

Due to the change in writing with complex numbers the rule for calculating intensity from a field intensity now is:

$$I = E \cdot E^*$$

in which case E^* is the conjugate-complex of E (Rule: exchange i with $-i$). The following sum of individual field intensities must now be calculated:

$$E = \text{Re} \left\{ e^{i(\omega t + kx)} \cdot \sum_{n=1}^p A_n \cdot e^{i(n-1)\delta} \right\}$$

Inserted for A_n and $e^{-i\delta}$ from the sum of $n=1$ till p reflections taken out:

$$E = \text{Re} \left\{ e^{i(\omega t + kx)} \cdot (1-R) \cdot A_0 \cdot \sum_{n=1}^p R^n \cdot e^{i(n-1)\delta} \right\}$$

$$E = \text{Re} \left\{ e^{i(\omega t + kx)} \cdot (1-R) \cdot A_0 \cdot e^{-i\delta} \cdot \sum_{n=1}^p R^n \cdot e^{in\delta} \right\}$$

The sum shows a geometric series, the result of which is:

$$\sum_{n=1}^p R^n \cdot e^{in\delta} = \frac{1-R^p \cdot e^{ip\delta}}{1-R \cdot e^{i\delta}}$$

For the electric field strength E we get:

$$E = \text{Re} \left\{ e^{i(\omega t + kx)} \cdot (1-R) \cdot A_0 \cdot e^{-i\delta} \cdot \frac{1-R^p \cdot e^{ip\delta}}{1-R \cdot e^{i\delta}} \right\}$$

If we now increase the reflections p to an infinite number, R^p will go against zero since $R < 1$ and the result is:

$$E = \text{Re} \left\{ e^{i(\omega t + kx)} \cdot (1-R) \cdot A_0 \cdot e^{-i\delta} \cdot \frac{1}{1-R \cdot e^{i\delta}} \right\}$$

As already mentioned, the intensity is given by:

$$I = E \cdot E^*$$

$$I = I_0 \frac{(1-R)^2}{(1-R \cdot e^{i\delta}) \cdot (1-R \cdot e^{-i\delta})}$$

$$I = I_0 \frac{(1-R)^2}{1-R \cdot e^{i\delta} - R e^{-i\delta} + R^2}$$

$$I = I_0 \frac{(1-R)^2}{1+R^2-2R \cos \delta}$$

with

$$2 \cdot \sin^2 \left(\frac{\delta}{2} \right) = 1 - \cos \delta$$

we get:

$$I = I_0 \frac{(1-R)^2}{1+R^2-2R \cdot (1-2 \sin^2(\delta/2))}$$

and finally:

$$I = I_0 \frac{(1-R)^2}{(1-R)^2 + 4 \cdot R \cdot \sin^2(\delta/2)}$$

Let us now add the abbreviation for δ again and consider that for an infinite number of reflections either the angle of incidence α becomes zero or the mirrors have to be infinitely large. If α is set equal to zero, we get

$$\delta = \frac{2 \cdot d \cdot k}{\cos \alpha} = 2 \cdot d \cdot k$$

and the final result:

$$I = I_0 \frac{(1-R)^2}{(1-R)^2 + 4 \cdot R \cdot \sin^2 \left(\frac{2\pi d}{\lambda} \right)} \quad (7)$$

This function (shown in Fig. 5) was first derived by G.B. Airy (Philos.Mag. (3) Bd.2 (1833)).

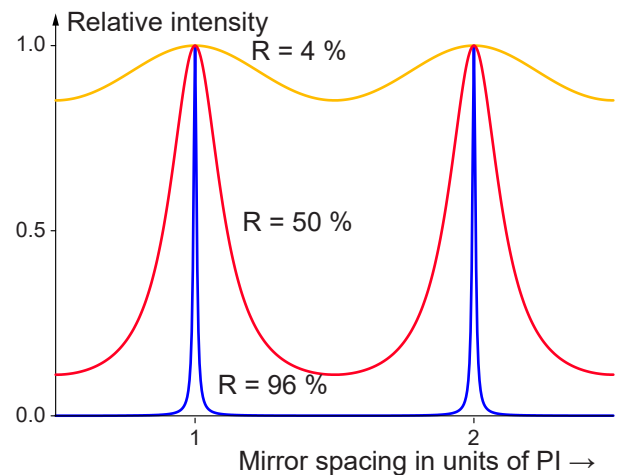


Fig. 5: The transmission curves of a Fabry Perot interferometer for different degrees of mirror reflection R

At first it appears astonishing that at the point of resonance where the mirror distances of the Fabry Perot are just about a multiple of half the wavelength, the transmission is 1, as if there were no mirrors there at all.

Let us take, for example, a simple helium-neon laser with 1 mW of power output as a light source and lead the laser beam into a Fabry Perot with mirror reflections of 96%.

The resonance obtained at the exit will also be 1 mW. This means that there has to be 24 mW of laser power in the interferometer because 4% is just about 1 mW. Magic? - no, not at all - This reveals the characteristics of the resonator in the Fabry Perot interferometer. It is, in fact, capable of storing energy. The luminous power is stored between the mirrors. This is why the Fabry Perot is both an interferometer as well as a resonator. It becomes a resonator when the mirror distance is definitely adjusted to resonance, as is the case, for example, with lasers. There are three areas of use for the Fabry Perot:

1. As a Length measuring equipment for a known wavelength of the light source. The Michelson interferometer offers better possibilities for this.
2. As a High-resolution spectrometer for measuring line intervals and line widths (optical spectrum analyser)
3. As a High quality optical resonator for the construction of lasers.

In the following series of experiments the Fabry Perot is used as a high resolution spectrometer to analyse the mode spectra of a probe laser. All the parameters required for understanding the Fabry Perot as a laser resonator are obtained within the following chapter and at the end of the chapter on the fundamentals, the most important parameters of the FP will be discussed, using the ideal FP as an example first, and secondly we illuminate the practical aspects, which reveals significant differences from the ideal behaviour of the ideal FP. Fig. 15 is shown to get an idea of the practical side in the introductory chapter itself.

We are looking at the spectrum analyser with the FP as shown in Fig. 6.

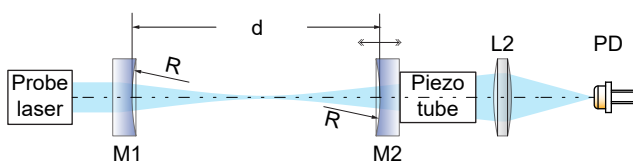


Fig. 6: Experimental situation

The FP is formed by two mirrors M1 and M2, fixed parallel to each other by adjustment supports. To the mirror M2 a piezo element is attached which allows the periodic variation of the mirror distance d of some μm by applying an electric voltage to the piezo element. The transmitted light of the FP is collected and imaged to a photo detector. A monochromatic probe laser with a small bandwidth is used as a light source. Linear changes in the mirror distance take place periodically and the signal is shown on an oscilloscope (Fig. 7).

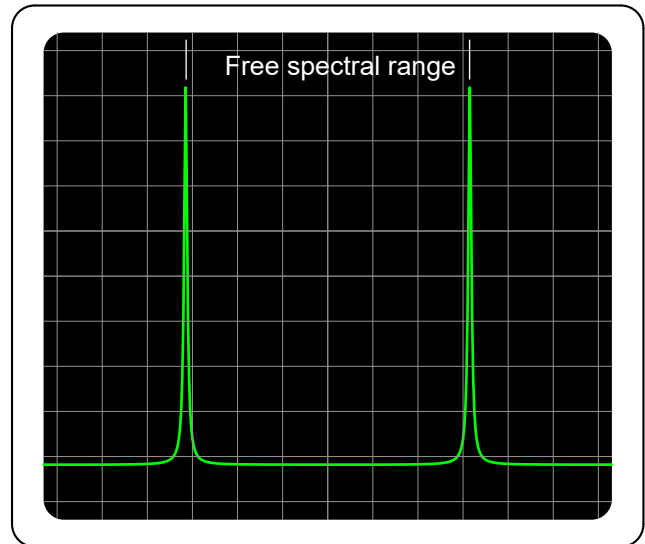


Fig. 7: Transmission signal on an oscilloscope with a periodic variation of the mirror distance d

The parameters of the FP are now be explained by using Fig. 7. Two transmission peaks can be seen. It is obvious that the distance d of the FP has been changed by $\lambda/2$. In our example we are using a He-Ne laser with the wavelength of 632 nm, so the change in distance was just over 316 nm or 0.000316 mm. The distance between the two peaks is defined as the:

Free Spectral Range FSR.

The value of the FSR depends on the distance d of the mirrors as shown below. For practical reasons, this distance will be given in Hz. The light wave is reflected on the mirrors of the resonator and returns back to itself. The electric field intensity of the wave at the mirrors is always zero (Metal or dielectric mirror). At a given distance d the mirrors can only form standing waves which have the field intensity of zero at both mirrors. It is obviously possible for several waves to fit into the resonator if an integer multiple of half the wavelength is equal to d . The waves, which fit into a resonator of a particular length are also called oscillating modes or just modes. If the integer has the value n , then all waves which fulfil the following equation will fit into the resonator:

$$d = n \cdot \frac{\lambda_1}{2}$$

The next neighbouring mode must fulfil the condition

$$d = (n+1) \cdot \frac{\lambda_2}{2}$$

The difference between the two equations above gives us:

$$n \cdot \frac{\lambda_1}{2} - (n+1) \cdot \frac{\lambda_2}{2} = 0$$

or

$$\lambda_1 - \lambda_2 = \frac{\lambda_2}{n} = \frac{\lambda_1 \cdot \lambda_2}{2 \cdot d}$$

$$\frac{\delta\lambda}{\lambda_1 \cdot \lambda_2} = \frac{1}{2 \cdot d}$$

and

$$\nu = \frac{c}{\lambda} \Rightarrow \delta\nu = c \cdot \frac{\delta\lambda}{\lambda_1 \cdot \lambda_2}$$

ν is the frequency and c the speed of light. The result for the free spectral range:

$$\delta\nu = \frac{c}{2 \cdot d} \quad (8)$$

The term $\delta\nu$ is also called the mode distance. In an FP with a length L 50 mm, for example, the free spectral range or mode distance is $\delta\nu = 3$ GHz.

We can also deduce, from the size of the free spectral range calculated above, that the FP in Fig. 6 was tuned to 3 GHz with the mirror distance at 50 mm. If we increase the distance of the FP mirror to 100 mm the size of the FSR between two resonance peaks is 1.5 GHz. Bearing in mind that the frequency of the He-Ne Laser ($\lambda = 632$ nm) is $4.75 \cdot 10^5$ GHz, a frequency change in the laser of at least $\Delta\nu/\nu = 3 \cdot 10^{-6}$ can be proved.

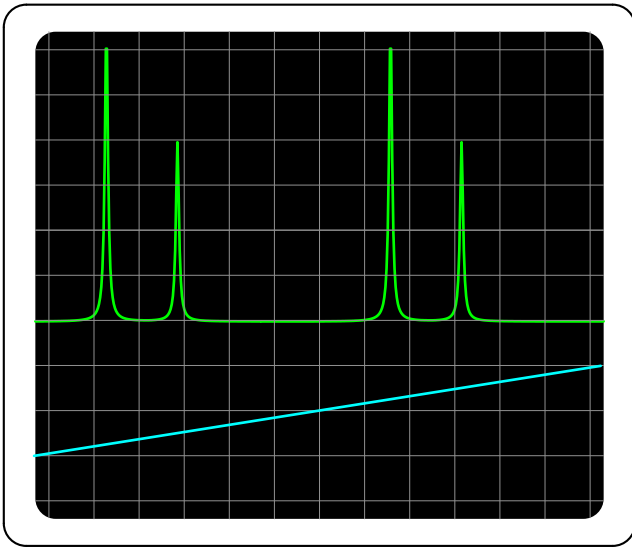


Fig. 8: Example of a scan of a two mode laser. The lower trace shows the change in length of the FP.

In the example shown in Fig. 8 the spectrum of a two mode laser was recorded. Two groups can be seen, consisting of two resonance peaks. Since the free spectral range, i.e. the distance between two similar peaks is known (through the measurement of the mirror distance and equation 8) the distance between the frequencies of two neighbouring peaks is also known and their difference in frequency can be measured precisely. Measurement of the absolute frequency with a Fabry Perot is, however, only possible if the exact mirror distance d is known. But this would involve considerable practical difficulties, since the determination of the length measurement would have to be accurate $< 10^{-6}$. At 50 mm this means $\delta d = \delta\lambda/\lambda \cdot 0.05 \text{ m} = 5 \cdot 10^{-8} \text{ m} = 50 \text{ nm}$!

A second important parameter of the Fabry Perot is its finesse or quality. This determines its resolution capacity. Fig. 5 shows the transmission curves for various reflection coefficients of the mirrors. There is clearly a connection between the width of a resonance peak and the value of reflection. It therefore makes sense to define the finesse as a quality:

$$F = \frac{FSR}{\Delta\nu}$$

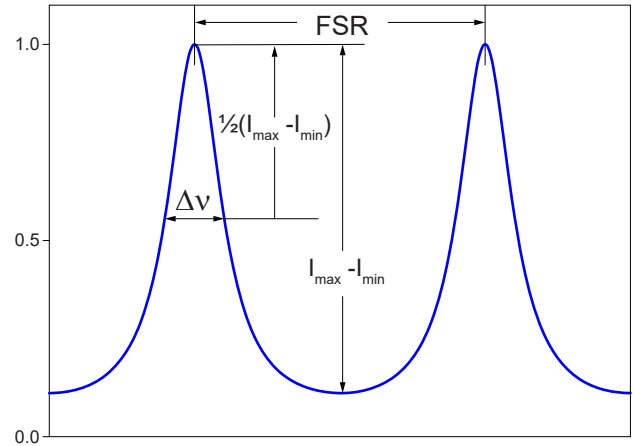


Fig. 9: Definition of finesse

For this purpose the full width at half maximum $\Delta\nu$ (FWHM) is calculated

$$I = \frac{I_{\max} - I_{\min}}{2}$$

Let us assume that $R \sim 1$. Then $I_{\min} \sim 0$ and

$$I = \frac{I_{\max} - I_{\min}}{2} \approx \frac{I_{\max}}{2}$$

or $I/I_0 = 1/2$. The values δ_1 and δ_2 can be calculated with Eq. 7 where the intensity is just about $1/2 I_0$.

$$\frac{I}{I_0} = \frac{1}{2} = \frac{(1-R)^2}{(1-R)^2 + 4 \cdot R \cdot \sin^2\left(\frac{\delta}{2}\right)}$$

$$(1-R)^2 + 4 \cdot R \cdot \sin^2\left(\frac{\delta}{2}\right) = 2 \cdot (1-R)^2$$

$$4 \cdot R \cdot \sin^2\left(\frac{\delta}{2}\right) = (1-R)^2$$

$$\sin\left(\frac{\delta}{2}\right) = \pm \frac{1-R}{2 \cdot \sqrt{R}}$$

$$\delta_1 = 2 \cdot \arcsin\left(\frac{1-R}{2 \cdot \sqrt{R}}\right)$$

$$\delta_2 = -2 \cdot \arcsin\left(\frac{1-R}{2 \cdot \sqrt{R}}\right)$$

since $(1-R) \ll R$, the function arcsin can be replaced by its argument:

$$\delta_1 - \delta_2 = 2 \cdot \frac{1-R}{\sqrt{R}}$$

with

$$\delta = k \cdot 2d = \frac{2\pi}{\lambda} \cdot 2d = \frac{2\pi\nu}{c} \cdot 2d$$

$$\delta_1 - \delta_2 = \frac{4\pi d}{c} \cdot \Delta\nu = 2 \cdot \frac{1-R}{\sqrt{R}}$$

$$\Delta\nu = \frac{c}{2\pi d} \cdot \frac{1-R}{\sqrt{R}}$$

and due to the definition

$$F = \frac{FSR}{\Delta\nu}$$

we get by substituting for F:

$$F = \frac{c \cdot \sqrt{R} \cdot 2\pi \cdot d}{2d \cdot c \cdot (1-R)} = \frac{\pi \sqrt{R}}{1-R} \quad (9)$$

As we have already assumed, the finesse depends on the reflectivity R of the mirrors. This is also shown in Fig. 5. The tendency now would be to bring the reflectivity R as close as possible to 1 to achieve a high finesse.

There are, however limitations in the finesse for the plane mirror of the Fabry Perot that has been discussed till now. These limitations lie in the imperfection of the mirror surfaces, which do not exist to a great extent in the spherical FP's yet to be discussed.

So, in the next chapter we intend to address these problems.

1.2 The real Fabry Perot

The finesse cannot be increased to over 50 even if a plane mirror of high technical precision is used. A finesse of 50 requires a flatness of $\lambda/100$ (λ approx. 500 nm) i.e. around 0.000005 mm = 5 nm !

This is because in anything other than an ideal plane mirror surface, the beams do not reflect back precisely, but they diverge from the ideal path in approximately thousands of rotations. This blurs the clear phase relationship between the waves and as a consequence the resonance curve becomes wider.

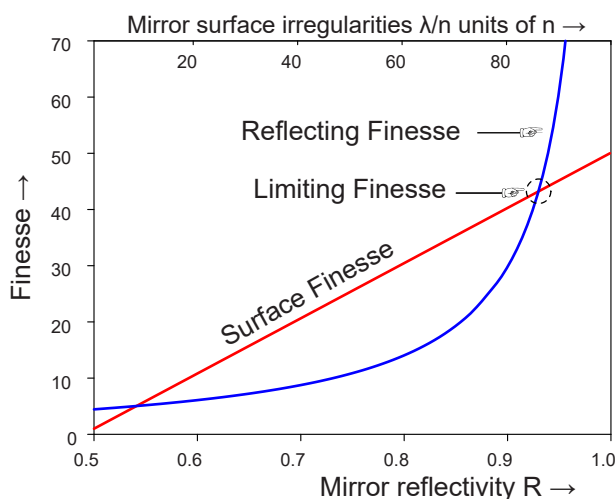


Fig. 10: Limitation of the finesse by the imperfect surface of the mirror of the Fabry Perot

If, on the other hand, spherical mirrors are used, then the occurrence of mistakes in sensitivity are much less. In the case of spherical FP's however, care must be taken that the diameter of the light falling in is smaller than the diameter of the mirrors. Generally speaking, this can be accomplished

particularly well in laser applications. Plane FP's have thus very little significance in laser technology.

1.3 The Spherical Fabry Perot

A spherical Fabry Perot consists of two mirrors with a radius of curvature r . The most frequently used FP is the confocal FP where the mirror distance L is equal to r (Fig. 11). The path difference δ is $4r$ for beams close to the centre. So, the free spectral range FSR ($\delta\nu$) is:

$$\delta\nu = \frac{c}{4 \cdot d} \quad (10)$$

But the spherical FP is not subjected to the limitations of a plane mirror in terms of total finesse based on divergences from the ideal mirror surface or maladjustment. If the mirror of a plane FP is tilted by the angle ε , the reflected beam is deflected by 2ε . Due to the imaging characteristic of spherical mirrors, maladjustment has a much lesser effect on the total finesse. The limiting finesse of a spherical FP is therefore mainly the reflection finesse. Moreover, spherical mirrors can be produced more precisely than plane mirrors.

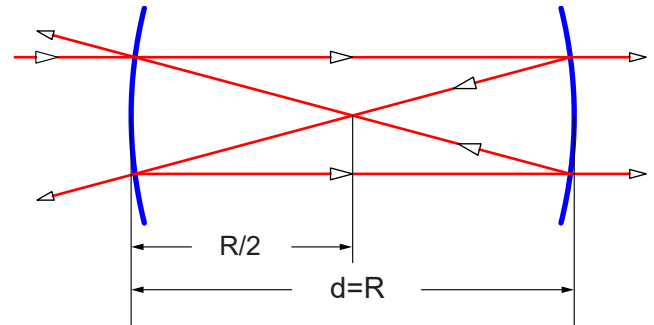


Fig. 11: Confocal Fabry Perot

1.4 The Spherical FP in practice

The first mirror of the FP acts as a plane-concave lens for the incident beam. Thus the path of the incoming beam inside the Fabry Perot is deviated as shown in Fig. 12. A biconvex lens enables the incoming beam to run parallel to the optical axis within the FP.

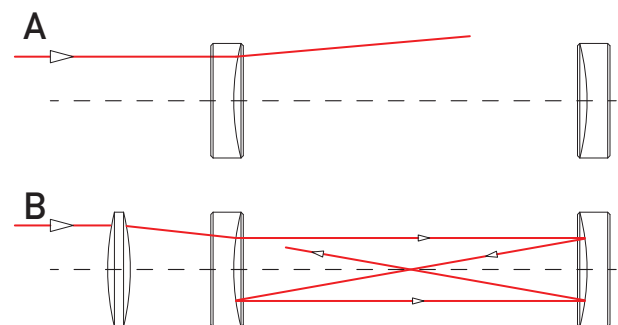


Fig. 12: A biconvex lens is recommended to make the incident beam run parallel to the optical axis

1.5 Optical Stability Criterion

Apart from the confocal FP, other types resonators with different mirror shapes can be created. As a necessary prerequisite, they must fulfil the criteria for stability.

$$0 \leq g_1 \cdot g_2 \leq 1 \quad (1)$$

A resonator can be considered as optical stable when the beam remains inside the mirror cavity after an infinite number of reflections. To calculate the stability range of a resonator we introduce the g-parameter as:

$$g_i = 1 - \frac{d}{R_i}$$

Hereby is d the distance between the mirrors and R the radius of the mirror. The Index i is for the left mirror 1 or for the right mirror 2. If the product $g_1 \cdot g_2$ sufficiently fulfils the above condition (1), the resonator is optically stable (Fig. 13). Various combinations of g_1 and g_2 can be combined in the shaded areas as far as the radius of curvature R and the mirror distance d are concerned with a more or less good finesse, representing the most important parameter for the FP when used as a spectrum analyser. The highest finesse is achieved with a confocal resonator (B). Here is $d = R$ and thus g_1 and g_2 are zero.

The plane FP (A) has g -values of 1 since R is infinite. Finally we can choose a concentric arrangement with a mirror distance of $d = 2 \cdot R$ and g -values of -1. This case has been marked by C.

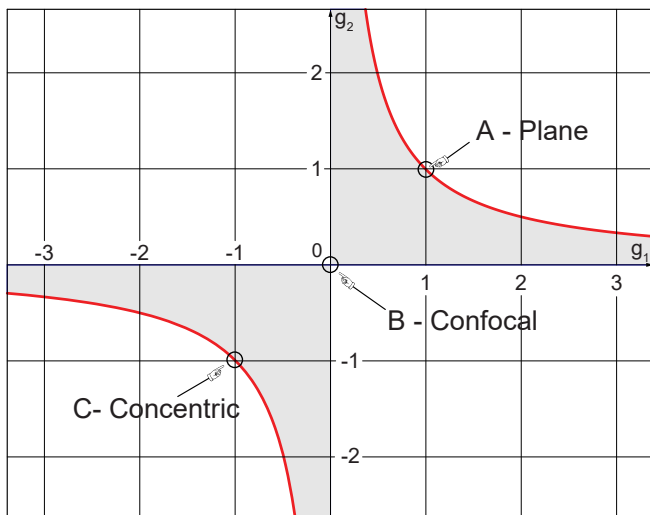


Fig. 13: Stability criterion of optical resonators

2.0 Experimental Setup

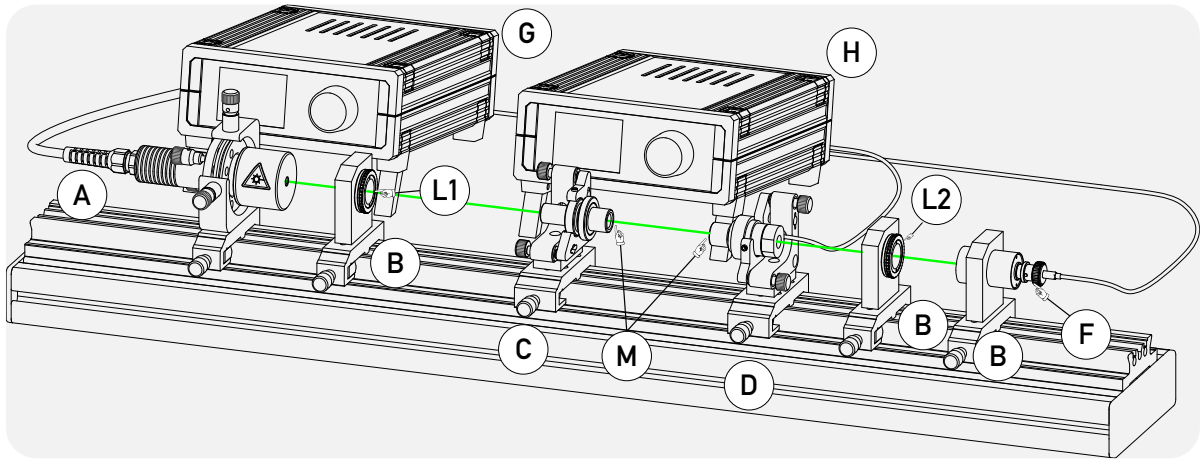


Fig. 14: Setup of the scanning Fabry Perot with a green emitting (532 nm) probe laser

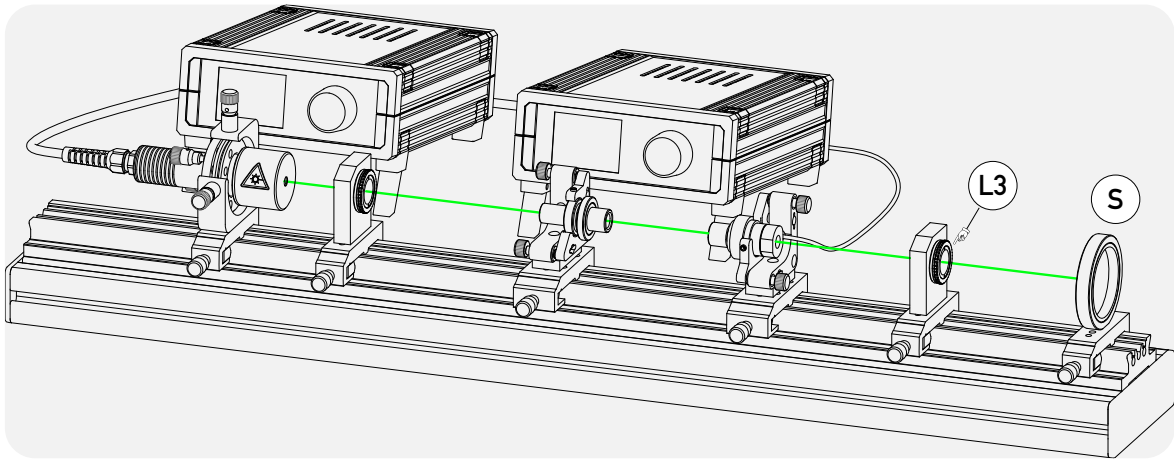


Fig. 15: Setup of the static Fabry Perot with a green emitting (532 nm) probe laser

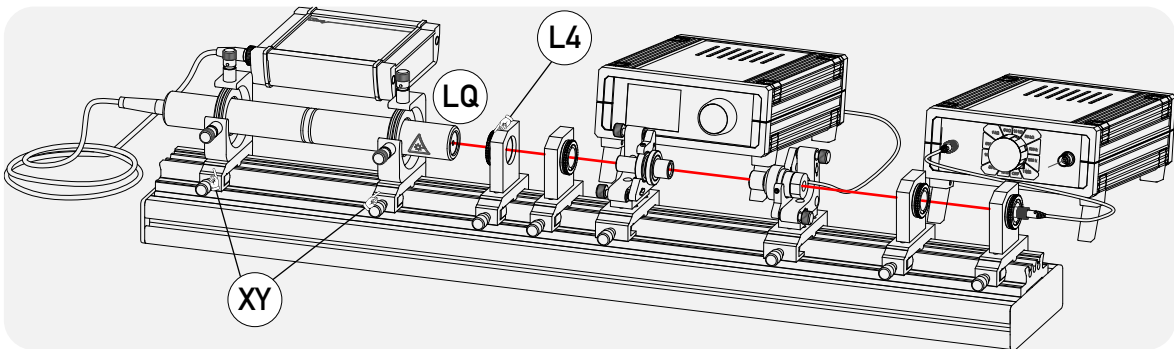


Fig. 16: Setup of the scanning Fabry Perot with a red emitting (632 nm) HeNe probe laser

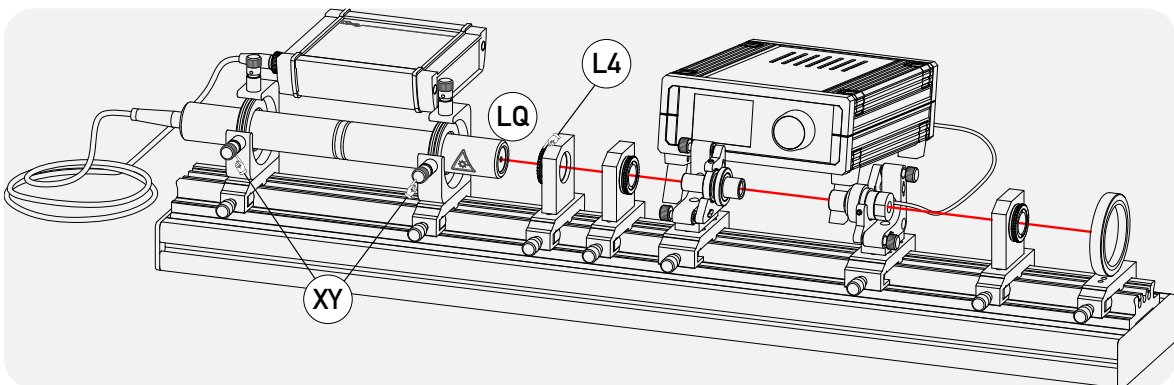


Fig. 17: Setup of the static Fabry Perot with a red emitting (632 nm) HeNe probe laser

2.1 Description of the components

- A Green (532 nm) stabilized Laser, 40 mW**
 In connection with the controller MK1-HP this laser module emits maximum 40 mW tunable 532 nm radiation in single mode with a frequency stability of ± 45 MHz. The green emitting DPSSL is mounted between two Peltier elements and the laser head is mounted into a 4 axes adjustment holder. Four precise fine pitch screws of repetitious accuracy allow the translational and azimuthal adjustment. The laser is connected to the controller with the 15 pin SubD HD connector which contains an EEPROM where the parameters of the laser are stored. The controller reads the data and sets the limiting values accordingly.



- B Mounting plate C25 on carrier MG20**
 This frequently used component is ideal to accommodate parts with a diameter of 25 mm where it is kept in position by three spring loaded steel balls. Especially C25 mounts having a click groove are firmly pulled into the mounting plate due to the smart chosen geometry. The mounting plate is mounted onto a 20 mm wide carrier.



- C Kinematic mount with axial translation on MG20**
 The kinematic mount is fixed to a 20 mm wide carrier MG20. It is equipped with an axial translation unit. It consists of a fixed body and a rotary insert. By turning this precisely manufactured insert a translation of 250 μm per turn is achieved. The rotary insert has a mount to accommodate components with a thread of M12x0.5.



- D Piezo transducer 10 μm /150V in kinematic mount**
 The transducer consists of a pre-loaded stack of piezo disks with a centre hole. The piezo disks are connected electrically in parallel, resulting in a displacement of 10 μm at 150 V. Typically 3 to 4 optical displacement orders require at a wavelength 500 nm a mechanical displacement of 1 μm . This is achieved by applying 15 volts only! This module combines the MM-0504 piezo transducer with a kinematic mount onto a 20 mm wide carrier MG20.



- L1 Biconvex lens f=150 mm in C25 mount**
 A biconvex lens with a diameter of 22 mm and a focal length of 150 mm is mounted into a C25 mount with a free opening of 20 mm.



- L2 Biconvex lens f=60 mm in C25 mount**
 A biconvex lens with a diameter of 22 mm and a focal length of 60 mm is mounted into a C25 mount with a free opening of 20 mm.



- L3 Biconcave lens f=-10 mm, C25 mount**
 A biconcave lens with a diameter of 10 mm and a focal length of -10 mm is mounted into a C25 mount with a free opening of 8 mm.



L4 Achromat f=20 mm in C25 mount

An achromatic lens with a focal length of 20 mm is mounted into a C25 mount with a free opening of 8 mm.



M Pair of mirrors M12

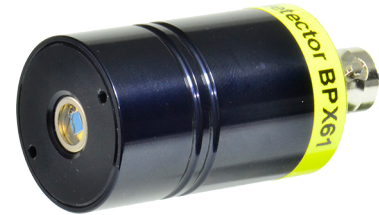
To attach the mirror to either the piezo electric element (D) or the kinematic mount with axial translation (C) it is mounted into a holder which fits to the M12 thread of D and C. By means of a threaded ring the mirror is pressed and centred against a soft rubber ring. Each of the provided mirrors has a transmission of 4% at 532 as well as 632 nm. Three different pairs of mirror with different radii of curvature (ROC) are available:

1. ROC 75 mm (standard)
2. ROC 100 mm (optional)
3. Flat mirror (optional)

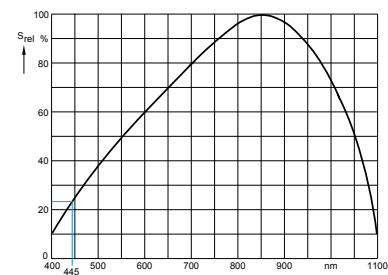


F Si PIN photodetector module (PD)

A Si PIN photodiode is integrated into a 25 mm housing with two click grooves (PD). A BNC cable and connector is attached to connect the module to the photodetector signal box ZB1. The photodetector module is placed into the mounting plate (MP) where it is kept in position by three spring loaded steel balls.



Parameter	Symb.	Value	Unit
Rise and fall time of the photo current at: $R_L=50\Omega$; $V_R=5\text{ V}$; $\lambda=850\text{ nm}$ and $I_p=800\ \mu\text{A}$	t_r, t_f	20	ns
Forward voltage $I_F = 100\text{ mA}$, $E = 0$	VF	1.3	V
Capacitance at $V_R = 0$, $f = 1\text{ MHz}$	C_0	72	pF
Wavelength of max. sensitivity	$\lambda_{S_{\max}}$	850	nm
Spectral sensitivity S 10% of S_{\max}	λ	1100	nm
Dimensions of radiant sensitive area	$L \times W$	7	mm ²
Dark current, $V_R = 10\text{ V}$	IR	≤ 30	nA
Spectral sensitivity, $\lambda = 850\text{ nm}$	$S(\lambda)$	0.62	A/W



Sensitivity curve $S_{\text{rel}}(\lambda)$

G Diode laser controller MK2-HP

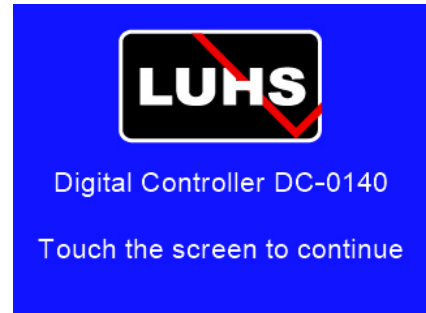
The diode laser module is connected via the 15 pin HD SubD jacket at the rear of the controller. The controller reads the EEPROM of the laser diode and sets the required parameter accordingly. The MK2 is powered by an external 12V/ 1.5 A wall plug supply. A USB bus allows the connection to a computer for remote control. Furthermore firmware updates can be applied simply by using the same USB bus. The central settings knob rotates a precision optical encoder to set the temperature, injection current and modulation frequency. The MK2 provides an internal modulator which allows the periodic switch on and off of the diode laser. A buffered synchronisation signal is available via the BNC jacket (MOD). The controller is equipped with a touch panel display and industrial highly integrated circuits for the bipolar Peltier cooler as well as for the injection current and modulation control of the attached laser diode. The injection current is stabilized within $\pm 1\text{ mA}$ and the diode laser temperature within $\pm 0.01\text{ }^\circ\text{C}$.



- G1** Upon switching on the controller, the main screen appears. The connected laser is probed.



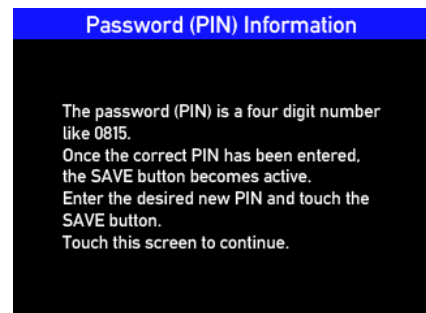
When the probing was successful, the touch on the screen continues to the password screen.



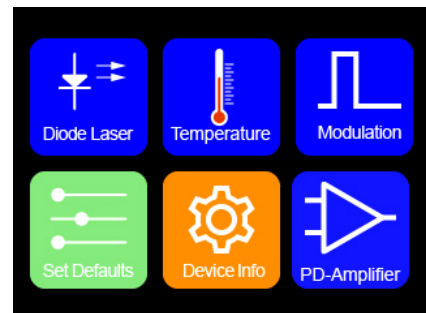
- G2** The upcoming interactive screen requires the log in to the device since due to laser safety regulations unauthorized operation must be prevented. In general this is accomplished by using a mechanical key switch. However, this microprocessor operated device provides a better protection by requesting the entry of a PIN. After entering the proper key the main screen is displayed and the system is ready for operation. The device comes with a default PIN, which can be changed once the log in with the default password was successful.



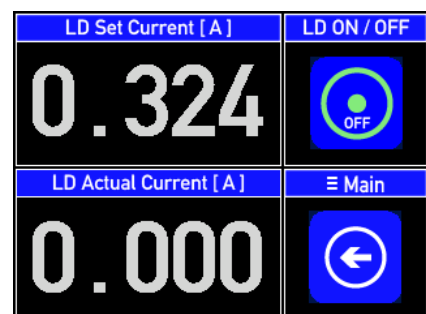
- G3** To get help for the change of the password touch the “How To” button on the top right of the screen.



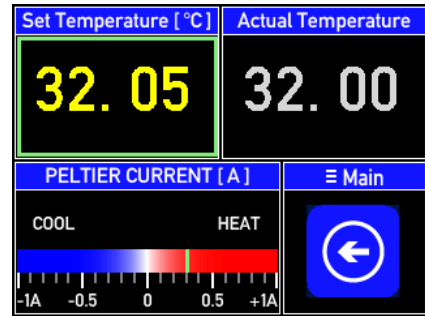
- G4** After successful log in the main screen appears with the selection of 6 buttons:
1. Diode Laser current settings
 2. Temperature settings of the diode laser
 3. Modulation of the diode laser
 4. Reset to default parameter
 5. Information about the connected laser and the controller itself
 6. Photodiode settings



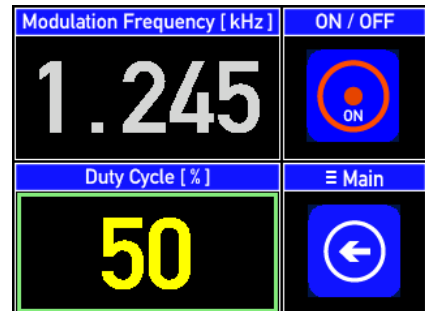
- G5** The diode laser current settings screen shows the set current as well as the actual current. By means of the LD ON/OFF touch button the laser is switched on or off. The Main touch button switches back to the main page back. By turning the knob, the value of the injection current can be set and is immediately applied, provided the LD ON/OFF touch button is activated. In this case the actual current is displayed.



G7 Selecting from the Main screen the temperature settings, the screen as shown in the right comes up. Touching into the “Set Temperature“ display field activates the setting knob and the desired value can be chosen. The selected value is immediately transferred to the high precision temperature controller. To keep the single mode of the green emitting laser stable an accuracy of ± 0.01 °C is required. The temperature can be set in a range from 10°C to 50°C and is accomplished by a Peltier element which can be heated or cooled and the current of the Peltier element is displayed in a bar graph representation.



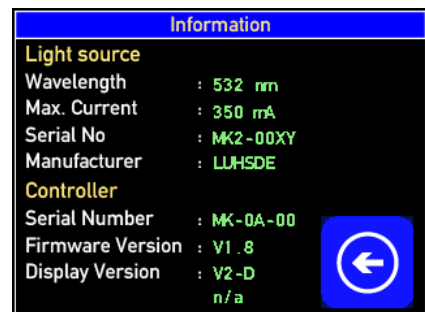
G8 A modulation of the injection current is not required within this experiment, but maybe useful for other applications. The modulation frequency as well as the duty cycle can be set.



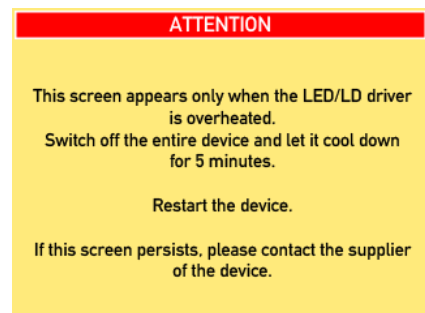
S9 This screen appears only, when no laser is connect to the device.



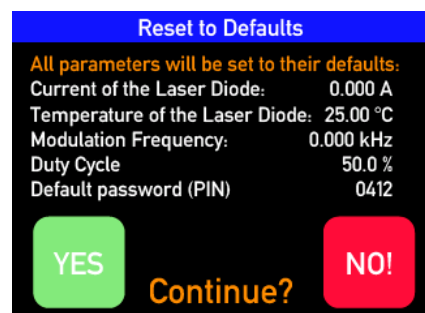
S10 The diode laser module is connected via the 15 pin HD SubD jacket at the rear of the controller. The controller reads the EEPROM of the laser diode and sets the required parameter accordingly. This information and some more information about the controller are shown on this screen.



S11 This screen you should never see. It appears only when the chip of the injection current controller is over heated. Switch off the device, wait a couple of minutes and try again. If the error persists please contact your nearest dealer.



S12 This screen provides the possibility to quickly reset the parameter (including the password)



G12 This screen provides the photodiode settings
The photodiode page displays the measured photo voltage, the selected shunt resistor and the chosen gain.

Tapping the gain display field switches the gain to 1, 2, 4 and 8.

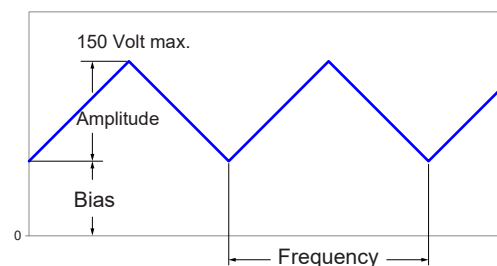
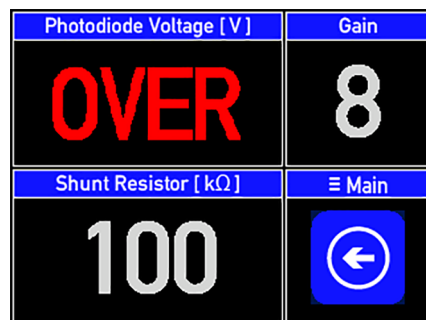
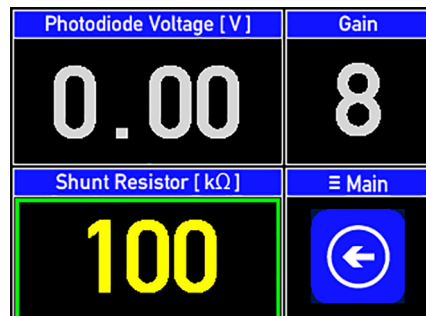
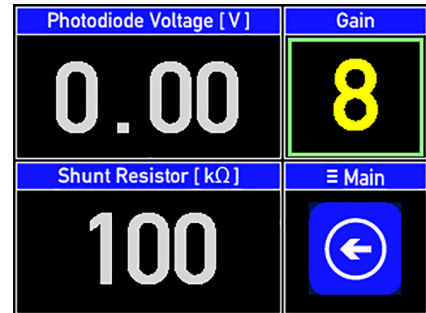
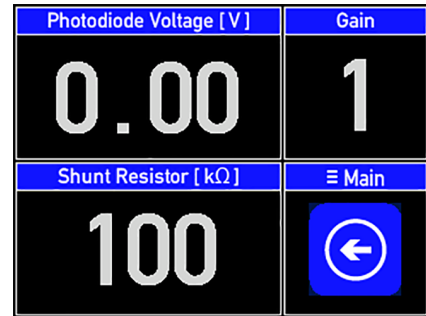
Activating the shunt resistor display field lets one set the shunt resistor by turning the digital knob. The value ranges from 1 kOhm to 200 kOhm.

If the photo voltage exceeds the inter reference voltage of 2.048 V the display shows the overload state. Reduce the gain or the shunt resistor. If the overload state remains although both values are set to minimum values, the injection current should be reduced as well.

H Piezo controller 0-150V

All voltages necessary for the supply of the Piezo element and all monitor signals are generated by this controller. The output voltage can be adjusted from 1 to 150 V and the frequency of the integrated modulator for triangular signals up to 100 Hz. A monitor signal which is proportional to the selected Piezo voltage is provided via a BNC panel jack at the rear. The controller is equipped with a touch panel display and in conjunction with the digital knob the parameter are selected and set.

To move the Piezo element periodically forth and back (to scan the Fabry Perot mirror spacing) a linear triangle shaped voltage is required. This voltage is characterised by the amplitude and its bias. The frequency should be chosen such, that a flicker free trace on the oscilloscope is achieved, a value of below 100 Hz is fully sufficient.

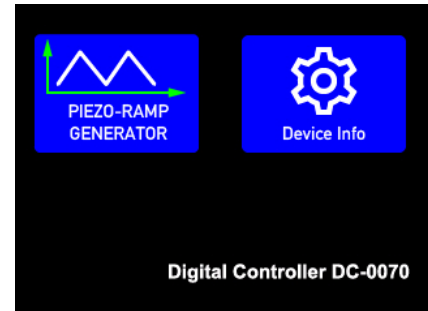


H1 Upon switching on the controller, the main screen appears. To continue it is required to touch the screen.

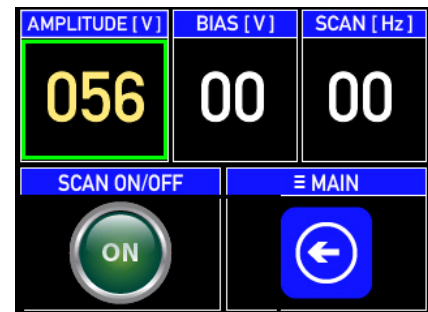


H2 The upcoming screen provides three touch buttons:

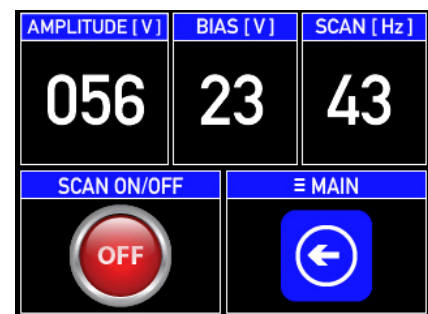
1. Piezo Settings
2. Device Info



H3 Within the “Piezo Settings” screen the piezo voltage can be switched ON or OFF. Touching the display area of the “Amplitude” it will be high lighted and with the setting knob the desired value is chosen. Touching the “BIAS” button display area activates the setting for this parameter. Touching the “SCAN” button area high lights it and allows the setting of the scanning frequency in a range from 1 to 100 Hz.



H4 Touching the “SCAN ON/OFF” button starts the periodic scan with the selected amplitude, bias and scan frequency. Please not that the Bias voltage is applied regardless the setting of the “SCAN ON/OFF” button. This is important when static experiments are performed.



P Photodetector Signal Box ZB1

The signal box contains a resistor network and a replaceable 9V battery and has an inbuilt photodiode to which an optical fibre with an FSMA thread is attached.

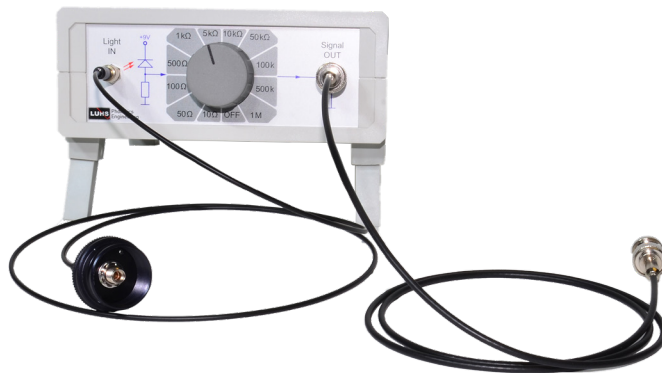


Fig. 18: Signal box DC-0300

At the output “Signal OUT” of the signal box a signal is present which is given by the following equation:

$$I_p = \frac{U_m}{R_L}$$

I_p is the photocurrent created by illuminating the photodiode with light.

U_m is the voltage drop across the selected load resistor R_L . To convert the measured voltage into a respective optical power we have to make use of the spectral sensitivity $S(\lambda)$ [A/W] which depends on the wavelength of the incident light according to . The detected optical power P_{opt} in W can be given as:

$$P_{opt} = \frac{I_p}{S(\lambda)}$$

Assuming a wavelength of 700 nm we take the value of S_{rel} from as 0.8 and subsequently the value of

$$S(\lambda=700nm) \text{ is } 0.62 \times 0.8 = 0.496$$

If we are measuring a voltage U_m of 1V with a selected resistor R_L of 1K the optical power will be

$$P_{opt} = \frac{I_p}{S(\lambda)} = \frac{U_m}{R_L \cdot S(\lambda)} = \frac{5}{1000 \cdot 0.496} = 10mW$$

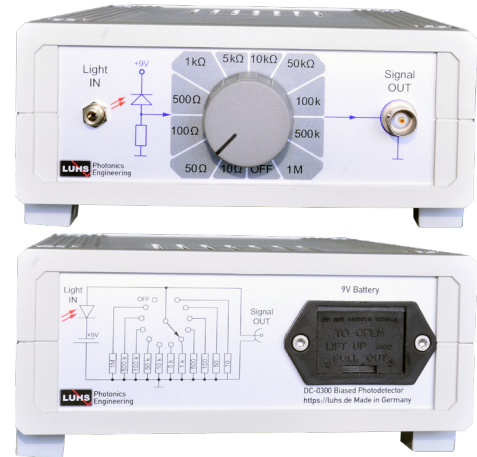
It must be noted that the measured power is correct only if the entire light beam hits the detector.

T Target Cross in C25 Mount

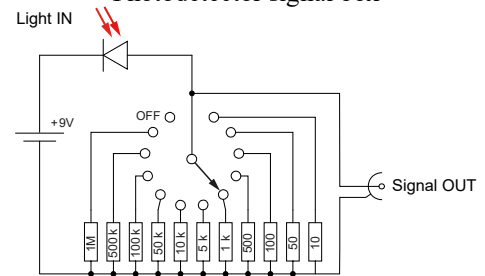
A crossed hair target screen is part of a 25 mm click holder C25 which can be inserted into the mounting plate (MP). The screen is kept in position by means of three precision spring loaded steel balls. It is used to visibly align a light beam with respect to the optical axis of the rail and carrier system.

S Translucent screen on carrier MG20

In a round holder a sheet of translucent paper is fixed with a retaining ring. This component is useful to image and visualize optical rays. Furthermore, the translucence allows the convenient photographic recording from the opposite side with digital cameras for a quick picture for the students measurement report.



Photodetector signal box



Photodetector signal box schematic

Based on the selected load resistor the sensitivity will be high for higher resistors but the rise and fall time will be longer. For fast signals a low resistor should be used, however the sensitivity will be lower.



LQ Two mode HeNe laser, 632 nm

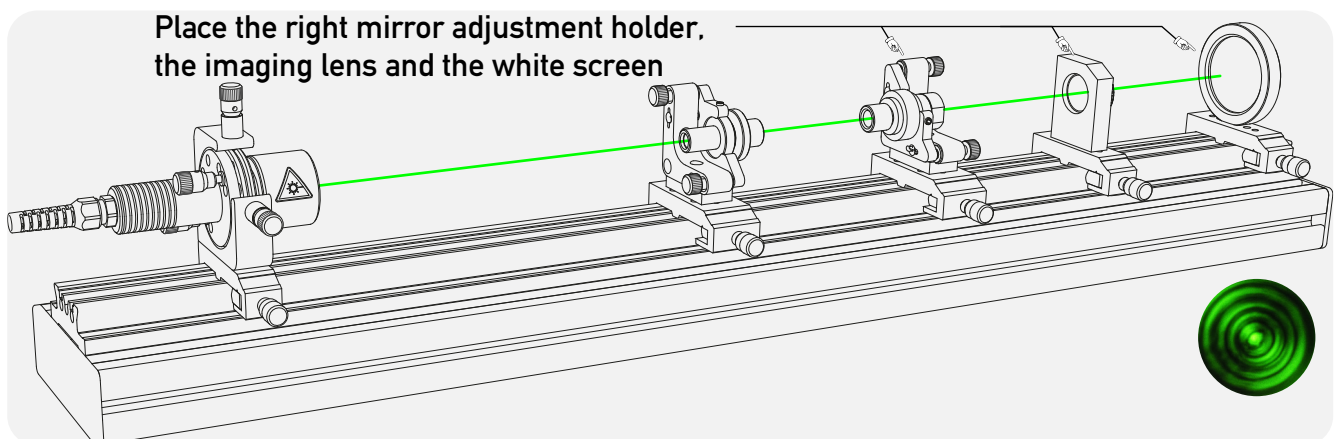
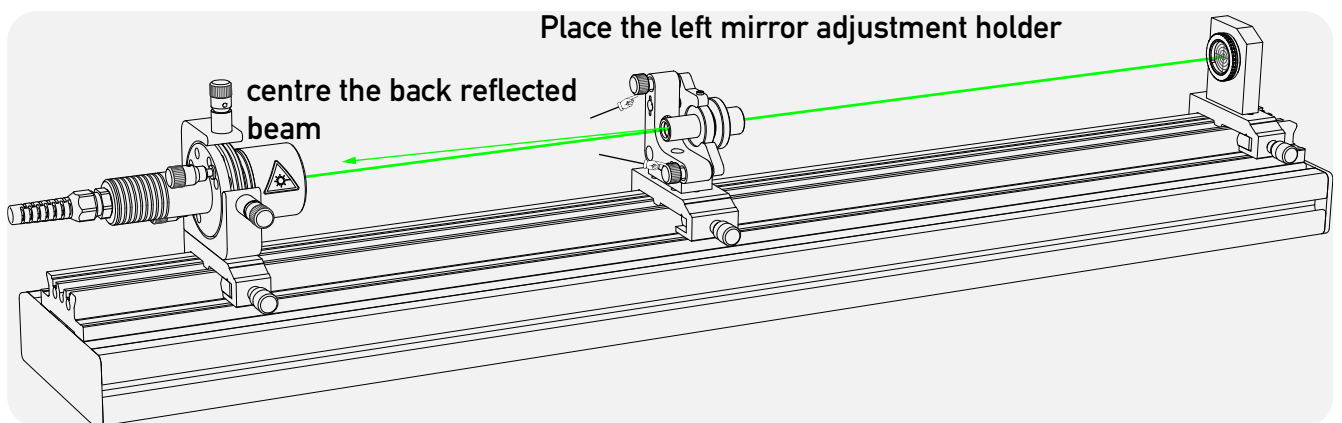
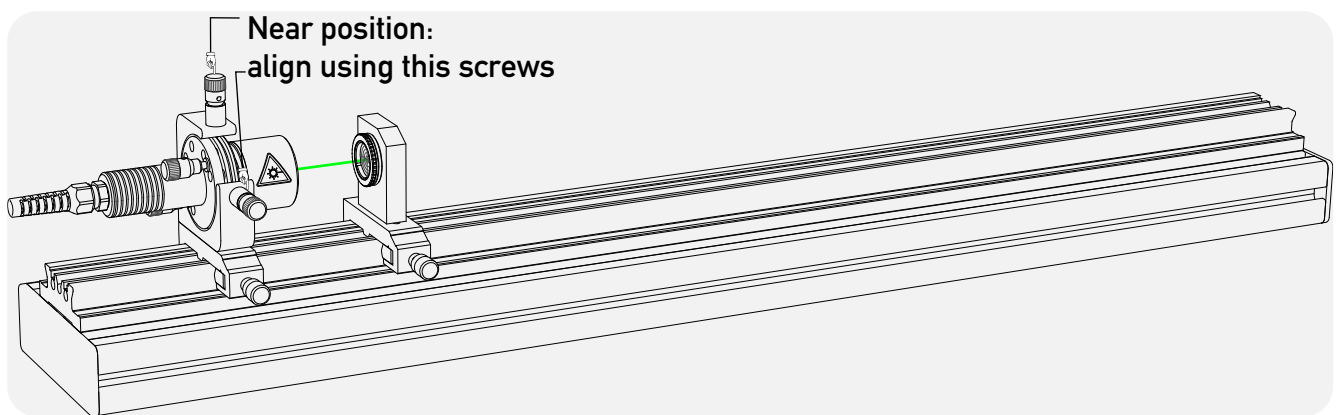
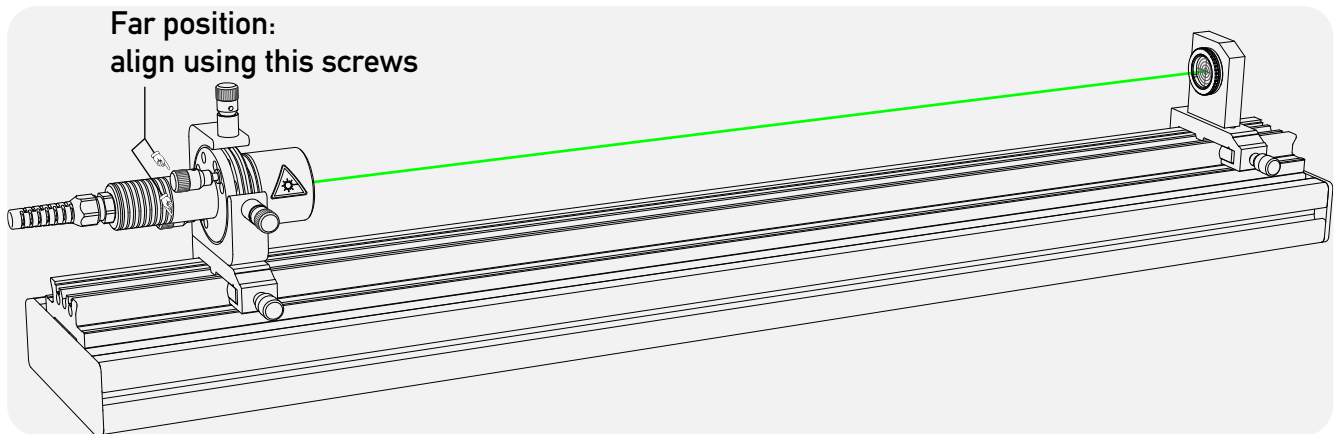
A helium Neon tube with a length of 18 cm is integrated into a black anodized aluminium housing with a diameter of 30 mm. Click grooves are applied to accommodate the tube either in a C30 mounting plate or in two XY adjustment mounts. The laser beam is precisely centred to the mechanical axis of the tube. The laser emits an output power of 1.5 mW at a wavelength of 632 nm and two orthogonal modes with a mode spacing of 900 MHz. For the operation of the tube, the power supply DC-0062 is provided.



DC-0062

3.0 Application and Measurements

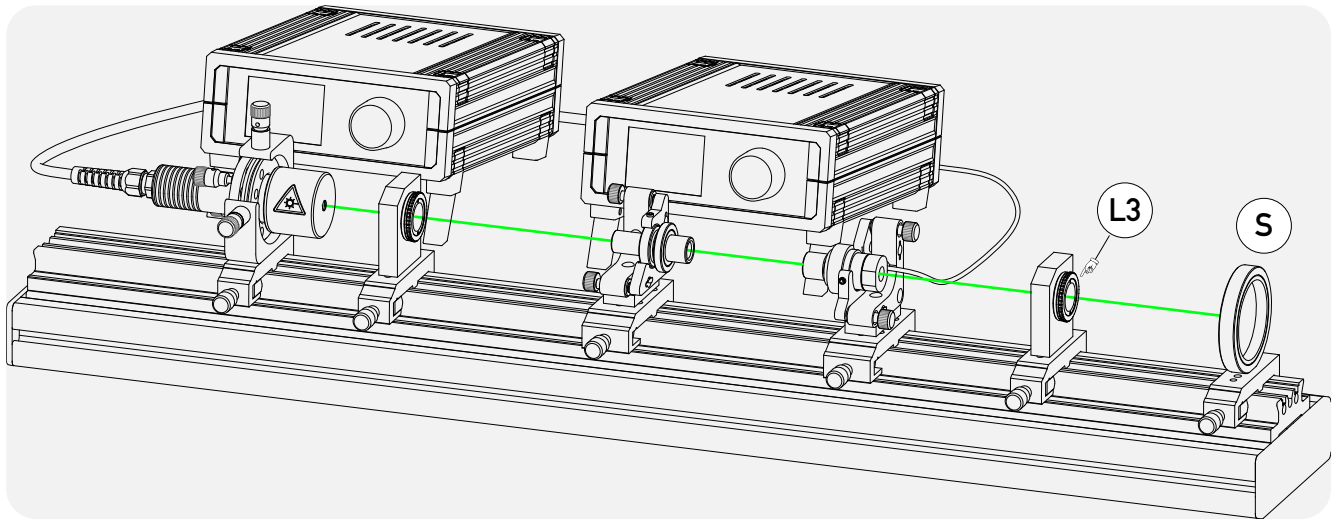
3.1 Experiments with the green emitting single mode laser



3.1.1 Static measurements

Once the right mirror adjustment holder is placed onto the rail, its distance to the left mirror should not exceed the radius of curvature (ROC) of the used mirror. If the mirror has for instance a ROC of 75 mm, this distance should be a little less than 75 mm. On the white screen interference fringes

appear and their structure depend on the alignment of the right mirror and the distance of both mirror. Reducing the distance by a couple of cm, more and more fringes appear. Realignment both the mirrors will yield a nice pattern.



Connect the piezo element to the controller and change the Bias voltage by hand. That will start moving the fringes. It is even more exciting setting the ramp frequency to 1 Hz and observe the fringes' movement.

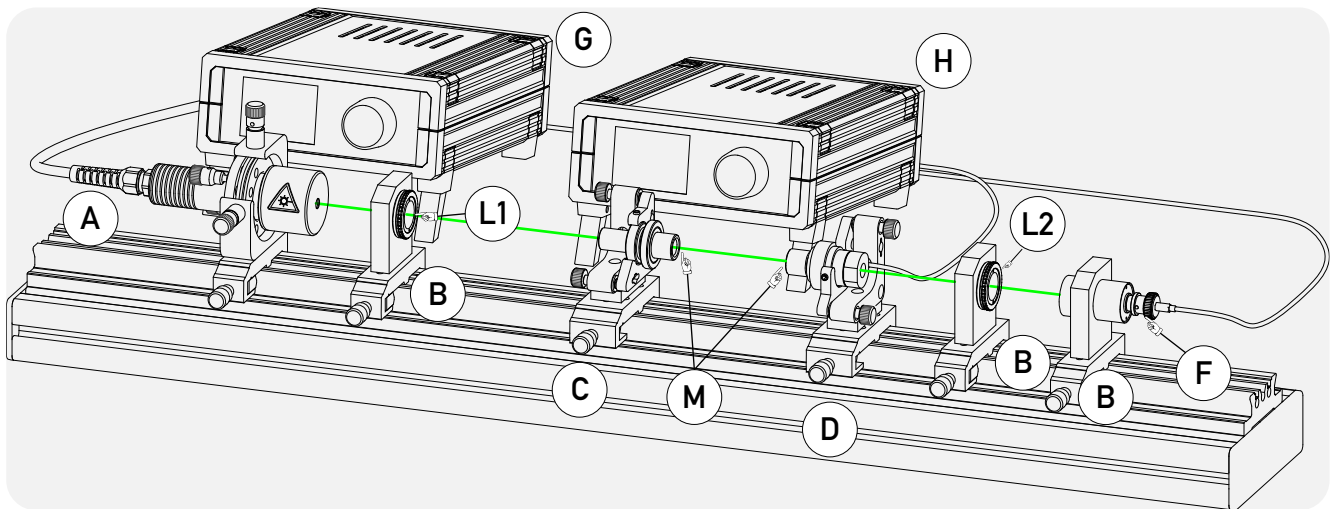


Fig. 19: Fabry Perot with photodetector to take the dynamic interference pattern

3.1.2 Dynamic Measurements

By exchanging the expanding lens (L3) with the focusing lens (L2) with a focal length of 60 mm and replacing the translucent screen (S) with the mounting plate (B) including the photodetector (F) the setup is ready for dynamic measurements. The photodetector (F) is connected to the controller (G). The photodiode signal from the controller is connected via the provided BNC cable to an oscilloscope. In the same way the PZT voltage reference signal is connected to the second channel of the oscilloscope and serves also as trigger source. At the beginning most likely a mode spectrum shown in Fig. 20 will be obtained. It shows a number of transverse extra peaks beside the main longitudinal mode. The transverse modes do not stem from the probe laser, they are ei-

genmodes of the Fabry Perot. These modes vanish once the confocal case is aligned and the cavity axis is collinear to the incident probe laser beam. The Fig. 21 shows the oscilloscope image of a well aligned confocal Fabry Perot. The FSR $\delta\nu$ for the confocal Fabry Perot is given by $\delta\nu = c/4R$ which yields for a radius of curvature $R=100$ mm of the mirror of a value 750 MHz. From Fig. 21 we further estimate the finesse of about 50 and a line width (FWHM) of 15 MHz. From this point we can conclude, that the line width of the probe laser is ≤ 15 MHz. The coherence length L_c of a laser source is related to $L_c = c/\Delta\nu$ with c as speed of light and $\Delta\nu$ the line width yields 20 metre, which is an astonishingly large value for a green laser pointer!

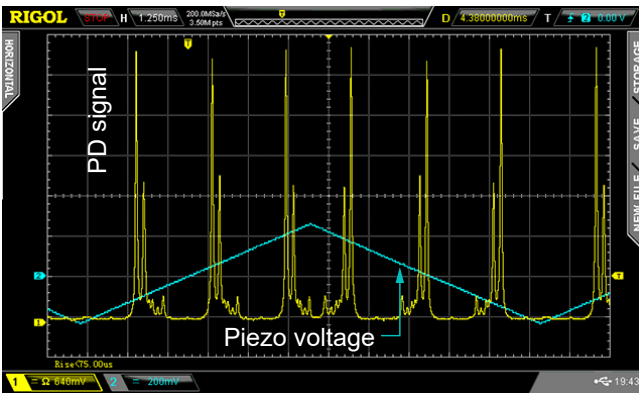


Fig. 20: Mode spectrum with transverse modes

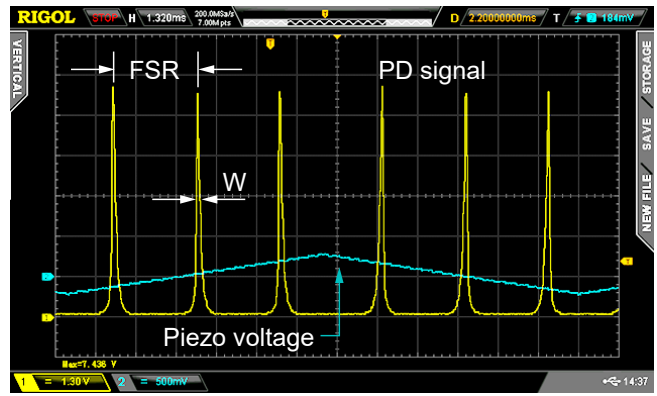


Fig. 21: Pure Single mode spectrum of the green probe laser

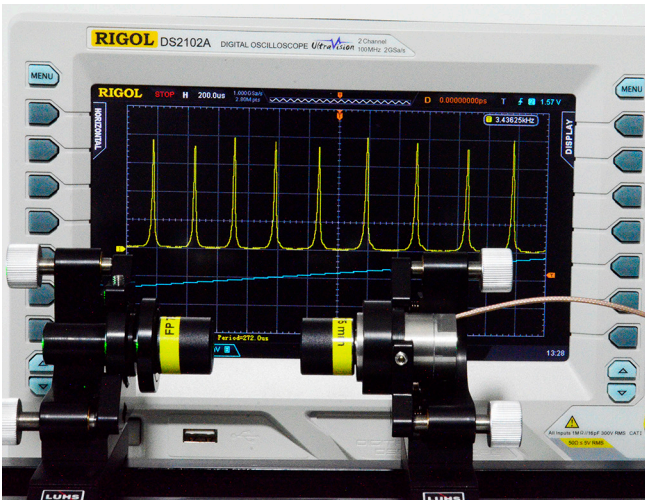


Fig. 22: Measurement with different mirror distances, however, with same ROC of 75 mm

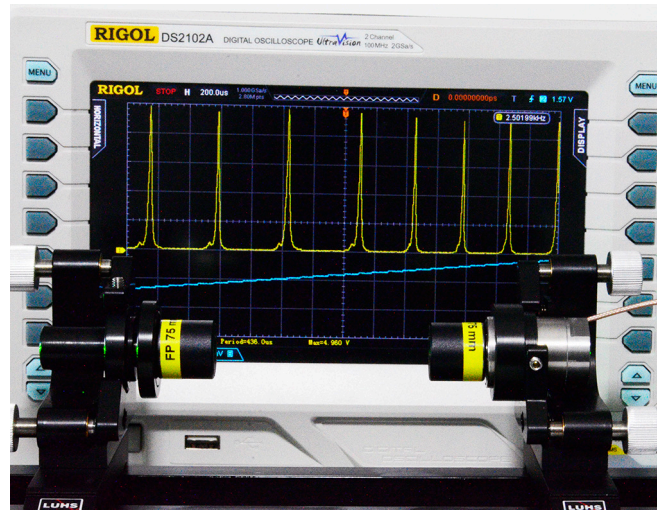


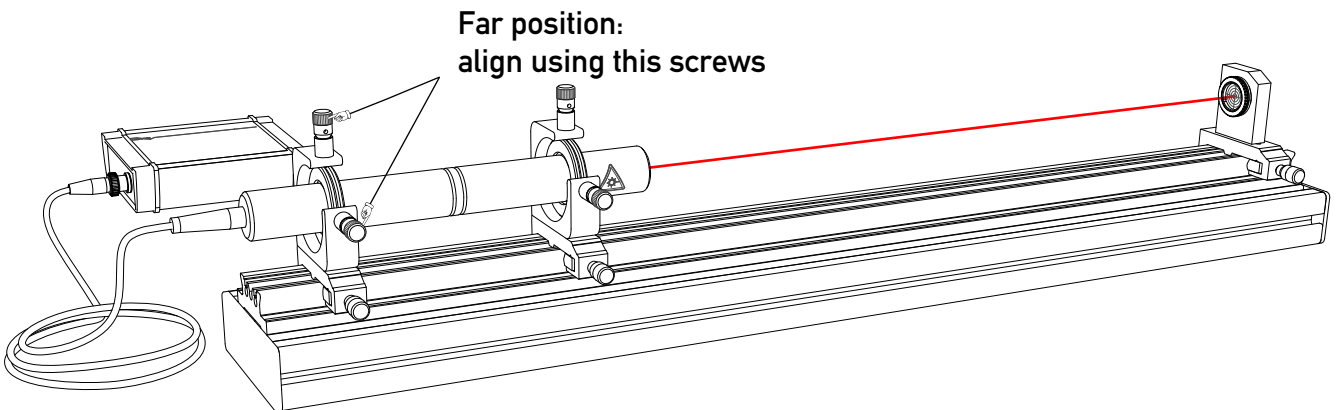
Fig. 23: Same measurement as the one as shown on the left, however the mirror distance d is ROC=75 mm

Helpful tips

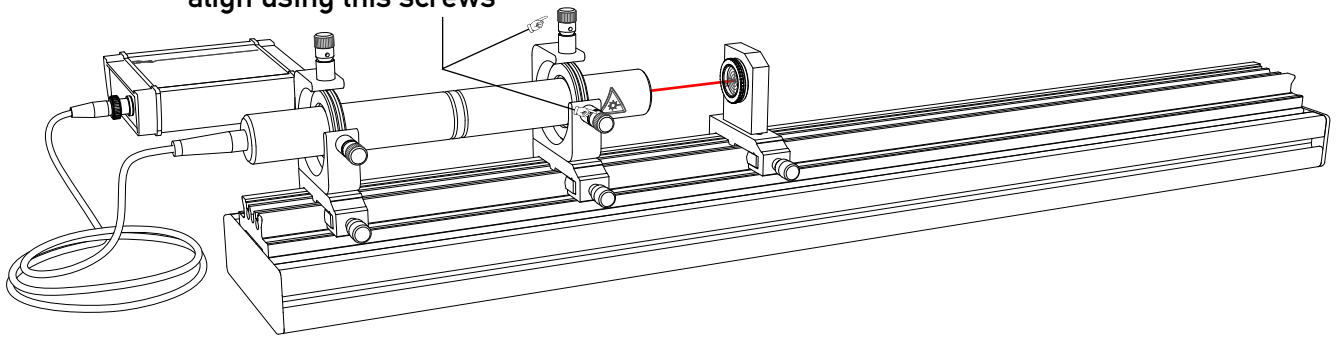
If you do not observe a clear structure on the oscilloscope, change the injection current and the temperature of the DPSSL. Values of 300 mA and 20°C appeared as good values. They may vary from laser to laser. Smoothly change the injection current and watch the oscilloscope until the clearest

pattern has been obtained. If still not a satisfactorily pattern is observed, optimize the mirror distance by successive turning of the left mirror by a quarter turn and realign the mirror for best peak appearance. After a while scope pictures as shown above should appear.

3.2 Experiments with the red emitting two mode HeNe laser

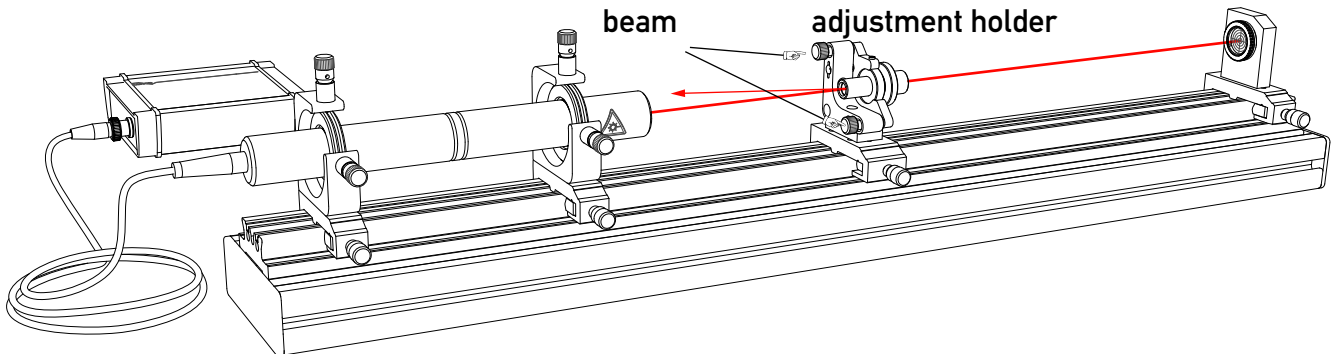


Near position:
align using this screws

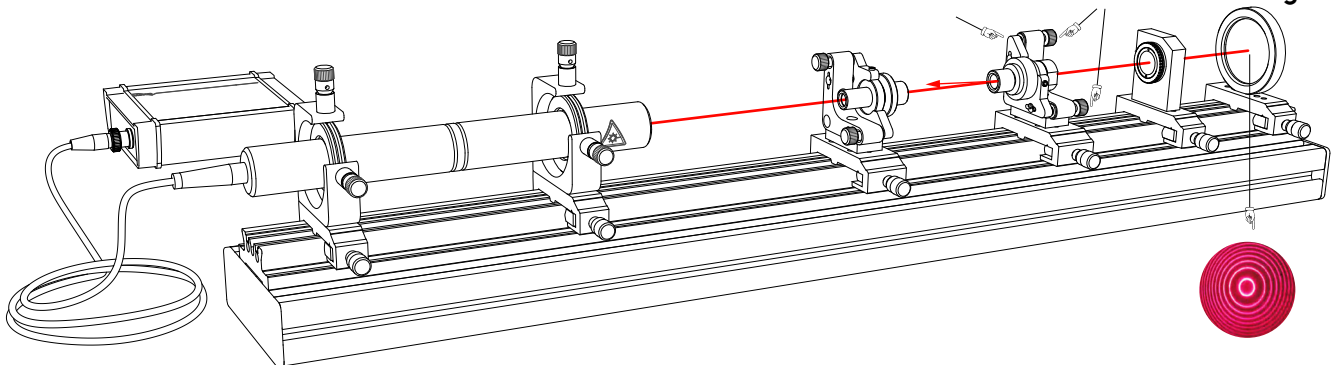


centre the back reflected
beam

Place the left mirror
adjustment holder

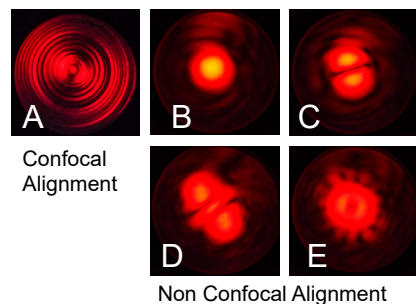


Place the right mirror adjustment holder Center back reflected light



3.2.1 Static measurements

Once the right mirror adjustment holder is placed onto the rail, its distance to the left mirror should not exceed the radius of curvature (ROC) of the used mirror. If the mirror has for instance a ROC of 75 mm, this distance should be a little less than 75 mm. On the white screen interference fringes appear and their structure depend on the alignment of the right mirror and the distance of both mirror. Reducing the distance by a couple of cm, more and more fringes appear. Realigning both the mirrors will yield a nice pattern.



Confocal
Alignment

Non Confocal
Alignment

3.2.2 Dynamic Measurements

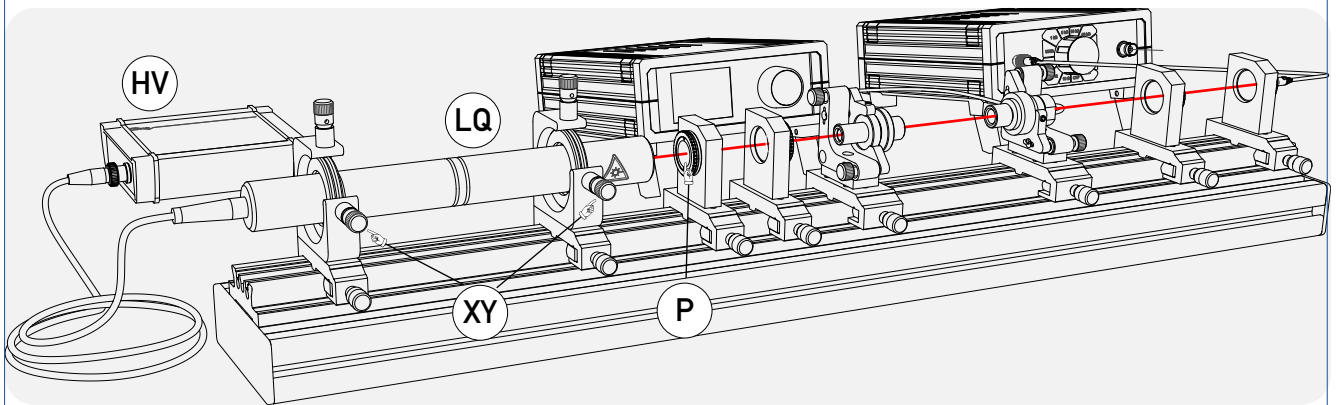


Fig. 24: Setup for dynamic measurements with the HeNe Laser

The extension kit comes with a two mode HeNe-laser (LQ) which is mounted into the two XY fine adjustment holder (XY). Soft silicon rubber O-rings keep the HeNe-laser tube in position allowing beside the XY translation also a tumbling motion. The necessary high voltage for the operation of the HeNe-laser is provided by the power supply (HV). Due to the larger dimensions of the HeNe-laser a 800 mm long optical rail (5) is provided. For the demonstration of the linear and orthogonal polarised modes a polarizer and a holder with a scale is provided (P). All other components are the same as used within the LM-0300 Fabry Perot experiment. Since the mirrors are coated for 532 nm as well as for 632 nm there is no need for extra mirror to operate the Fabry Perot with the red line of the HeNe-Laser. Once aligned, a mode spectrum as shown in Fig. 26 is obtained. The spectrum has been taken

with the 75 mm mirror set. Consequently the free spectral range (FSR) is 1 GHz. A pair of modes appear and depending on the warm-up state of the laser tube these modes are wander and change their amplitude. Two different mode spacings Δv can be identified:

$$\Delta v_1 = 295 \text{ MHz and } \Delta v_2 = 729 \text{ MHz}$$

At this point it becomes clear that a Fabry Perot cannot measure absolute values and one has to know something more about the probe laser. The HeNe-laser has a Doppler broadened profile with a gain width of 1.5 GHz. With the Fabry Perot we observe only two modes. If we assume the mode spacing Δv_1 is the correct one, then we have to expect 5 modes ($1.5 \text{ GHz} / 0.295$) which obviously is a contradiction to the measurement. Actually Δv_2 is the correct value, indeed the manufacturer specifies 730 MHz.

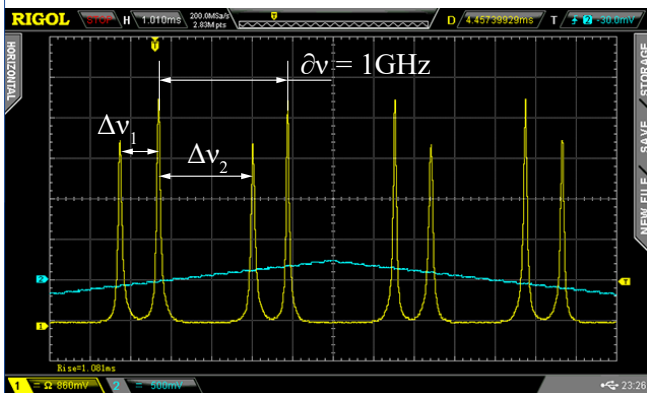


Fig. 25: FP with 75 mm mirror

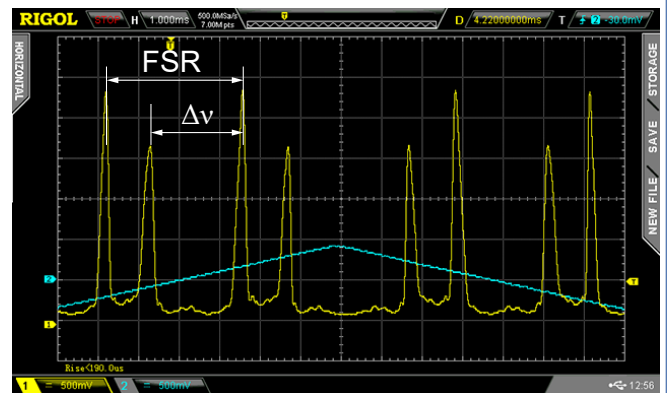


Fig. 26: Determining the frequency spacing of the two modes of the HeNe laser

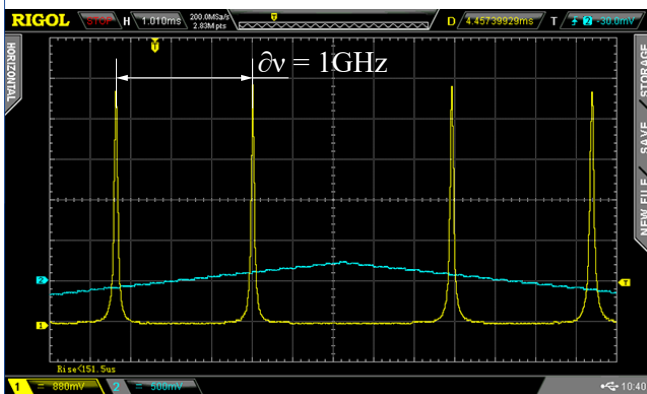


Fig. 27: Using the polarizer (P) to suppress one of the two modes of the HeNe laser. This impressively demonstrates that the two modes are orthogonally polarized to each other

